Street-level Heat and Air Pollution Exposure Informed by Mobile Sensing

Irfan Batur[1*] (ibatur@asu.edu)
Samuel A. Markolf[2] (smarkolf@ucmerced.edu)
Mikhail V. Chester[1] (mchester@asu.edu)
Ariane Middel[1] (ariane.middel@asu.edu)
David Hondula[1] (david.hondula@asu.edu)
Jennifer Vanos[1] (jenni.vanos@asu.edu)
[1]*Arizona State University, Tempe, Arizona, USA*
[2]*The University of California-Merced, Merced, California, USA*

ABSTRACT

Heat and air pollution persist as major public health hazards in urban environments. Yet there are gaps in the quality of information about the hazards as conditions tend to be informed by limited stationary sensors providing information at large geographic scales. Here we present the results of a study that took place in Phoenix, Arizona, to assess the efficacy of low-cost mobile sensors on public transportation vehicles to monitor fine-scale on-road heat and PM_{10} concentrations. The goal of the study is to uncover the spatial and temporal variations of excessive heat and air pollution experienced by transit commuters, bicyclists, and pedestrians. The results show that the sensors on the buses complement the readings from stationary sensors and low-cost mobile sensors are effective for gaining fine-grained heat and air quality readings at different locations, thereby creating new insights into pockets of heat and air pollution that should be targeted for intervention.

Keywords: Emerging Technologies, Active Transportation, Equity, Air Pollution, Extreme Heat

[*]Corresponding author.

1. INTRODUCTION

Heat and air pollution persist in urban environments as major public health hazards, and in many places are projected to worsen with population growth, climate change, or both. Research into the drivers of urban heat, and how people experience heat is increasing rapidly (Brandsma and Wolters, 2012; Karner et al., 2015; Nazarian et al., 2021). In the US, heat has been the top driver of weather-related fatalities for decades (National Weather Service, 2020). In the Southwest US, heat is a major public health hazard; there were 339 heat-associated deaths in Maricopa County, Arizona (Phoenix metro region) in 2021, 123 deaths in Clark County, Nevada (Las Vegas metro region) in 2017, and the State of California had on average 390 heat deaths per year between 2010 and 2019 (Maricopa County Public Health, 2021; Lupiani, 2021; Phillips et al., 2021). In Maricopa County, there are approximately 12 hospitalizations (morbidity) for every heat death (Eisenman et al., 2016). Heat and air pollution represent a concurrent and compounding hazard of major concern. Heat can alter atmospheric boundary layer conditions and air circulation in urban environments affecting air quality (Ichinose et al., 1999; Fan and Sailor, 2005; Makar et al., 2006; Lin et al., 2008; Chen et al., 2009). As people experience concurrent heat and air pollution, there are compounding negative physiological effects (Anenberg et al., 2020; Rahman et al., 2022). Taken together, there is growing concern about how climate change can impact public health at the nexus of heat and air quality.

Currently, air quality and heat are monitored by stationary sensors that are often dispersed across relatively large geographic areas. Although well-suited for providing a general understanding of air pollution and heat conditions across a region, this approach is somewhat limited in its ability to provide insights at the (hyper) localized scale at which people are exposed to and impacted by these hazards. In other words, the impacts of air pollution and extreme heat are experienced/felt at the "human scale," not the larger scales currently captured by existing monitoring networks (Steinle et al., 2013). There is a growing body of knowledge showing that both urban temperature and air quality can vary widely across space and time due to complex geographic, economic, ecological, and meteorological factors (Emmanuel and Fernando, 2007; Davis et al., 2010; Middel et al., 2014; Whiteman et al., 2014; Myint et al., 2015; Li et al., 2016; Mitchell et al., 2018). For instance, significant differences in temperature have been observed across and within neighborhoods in different urban areas (e.g., Kuras et al., 2015; Kuras et al., 2017; Middel & Krayenhoff, 2019). What is more, differences in meso- and microscale environmental conditions often converge with socio-economic conditions to disproportionately impact marginalized, under-represented, and underserved communities (e.g., Hondula et al., 2015; Karner et al., 2015). The spatial heterogeneity of environmental conditions (i.e., exposure to extreme heat and air pollution) and their potential impacts do not appear to be fully captured by the regional-scale monitoring and/or remote sensing approaches currently in practice. Therefore, novel approaches for understanding the circumstances of exposure to extreme heat and air pollution at a more refined scale appear warranted.

Many techniques – such as proximity models, interpolation models, land-use regression (LUR) models, dispersion models, and hybrid models – have been developed over time to quantify fine-scale spatial and temporal patterns of urban air pollution, meteorological conditions, and their source drivers (Jerrett et al., 2005; Shi et al., 2018; Viggiano et al., 2019). These methods characterize exposure levels at various scales and relate spatial patterns to major source sectors using a variety of modeling tools and data sources. They can also be integrated with other data sources, such as remote sensing data from satellite photos or geographical information system (GIS) data for validation and to provide new insights (Wu et al., 2018). Geostatistical interpolation models are most widely used to estimate spatially-explicit pollutant concentrations (e.g., Viggiano et al., 2019), while LUR models relate air pollution and weather conditions to various built environment attributes (Jerrett et al., 2005). Since both models require observations from monitoring sites, their exposure estimates are based on real-world data. Additionally, by considering local land use and traffic patterns at a specific site, LUR models offer an empirical framework for pollution and heat mapping. However, certain disadvantages are associated with using these models. Depending on the scale of the analysis and the study context, the models may require a dense network of sampling sites (Jerrett et al., 2005; Miller et al., 2020). Given the sparse network of government monitoring stations, accuracy of the estimations from interpolation and LUR models may be reduced, with potential difficulties such as over-smoothing the underlying patterns of microscale pollution or temperature variability, inaccuracies in estimates, and a lack of transferability to other geographic areas. To overcome these difficulties, primary data collection is often necessary but is challenging due to the high costs of operating and installing fixed monitoring sites.

Advancements in environmental and meteorological modeling offer one approach for gaining finer-scale insights into exposure to heat and air pollution. However, modeling and interpolation of environmental conditions can be subject to uncertainty, variability, and limitations in their applicability to different contexts due to the multitude of compounding urban conditions and dynamics that drive microclimates, as well as sensitivities to methodological assumptions and inputs (Oke et al., 2017; Hondula et al., 2018; Krayenhoff et al., 2021). Similarly, exposure models often assume that the entirety of an individual's exposure occurs at their home address or neighborhood, which is often inaccurate (Glass et al., 2015; Karner et al., 2015). This approach may be problematic as it does not fully account for the complexity of people's interactions with their environments across space and time and their physiological reactions to exposure and reprieve (Baxter et al., 2013). Towards generating critical insights into microclimate exposure, new techniques are needed to complement and supplement modeling efforts and regional-scale observational networks.

The growing ubiquity of accurate and low-cost temperature and air quality sensors presents an opportunity for novel methods to characterize microclimates and human exposure (Snyder et al., 2013; Kumar et al., 2015; Wang et al., 2021; Middel et al., 2022). For instance, there is an emerging body of work using sensors to measure the environmental conditions of individual persons as they conduct their daily activities (e.g., Kuras et al., 2015; Wang et al., 2021). However, despite exhibiting promise, these approaches are still faced with various challenges and limitations, namely scalability issues (i.e., recruiting and retaining participants across diverse communities and relatively long time periods), sensor limitations (McKercher & Vanos, 2018), and privacy concerns. Thus, we place an emphasis on mobile sensing, where vehicles are outfitted with sensors to capture environmental information across space and time at higher fidelity than stationary sensors (Hankey and Marshall, 2015; Mitchell et al., 2018; Miller et al., 2020). Mobile sensing is in a relatively nascent stage and only a few studies have assessed its accuracy and feasibility (Kumar et al., 2015; Xie et al., 2017; Li and Lau, 2018; Kaivonen and Ngai, 2020; Mallia et al., 2020; Van den Bossche et al., 2015; McKercher & Vanos, 2018).

Since weather and air quality conditions can change dramatically over small distances and/or in a short amount of time, mobile sensors mounted to vehicles allow for data collection in a variety of locations without incurring additional costs for sensor installation on city infrastructure (Kaivonen and Ngai, 2020). They also improve coverage and enable semi-continuous characterization of the fine-scale heterogeneity of temperature and emissions in the sensing area – outcomes that are difficult to achieve with existing observational and modeling approaches. As a result, hotspot detection, exposure monitoring, and high-resolution air quality and temperature mapping are possible with this technology (Elen et al., 2012). In deciding which vehicles to outfit with mobile sensors, urban public transit systems represent a constellation of preferable factors. The systems are public and therefore more easily accessible for placing sensors, have operations that cover the entire city, and are often serving population subgroups that experience higher vulnerability to heat and air pollution (Gil-Castiñeira et al., 2008; Jamil et al., 2015; Marjovi et al., 2015; Alsina-Pagès et al., 2016; Barri et al., 2021). Outfitting urban bus networks with environmental sensors represents a potentially significant advancement in our ability to understand and address microclimate variability and human exposure to extreme heat and air pollution – particularly in communities that are disproportionately impacted by these hazards.

Towards this end, we present approaches and results from a research effort in Phoenix, Arizona to test the efficacy of low-cost mobile air temperature and air pollution (specifically PM_{10}) sensors on public transit buses. In particular, we investigate the feasibility of creating a mobile sensing platform with public transit vehicles. We also explore the potential data and insights that this approach can provide with respect to identifying localized "hot spots" for extreme heat and air pollution, as well as informing the ability of decision-makers and community members to mitigate potential impacts from these hazards. To the best of our knowledge, this is the first study to use this approach to simultaneously examine temperature and air quality at the sub-neighborhood scale. We also help advance synergies between environmental sensing, vulnerability and risk analysis, transit and urban planning, and environmental equity/justice. Note, throughout the article we refer to collecting data and conducting analysis at the "human scale." We acknowledge that measurements from buses affixed with sensors are likely to be a few meters away from the conditions experienced by a person on the sidewalk or at the bus stop. Nonetheless, we feel that this phrasing helps convey the scope of our analysis and the actions/decisions it aims to inform.

2. METHODOLOGY

Low-cost temperature and air quality sensors were installed on public transportation vehicles to investigate the possibilities for increasing fine-scale monitoring of urban environments at the human scale. The study took place in the City of Phoenix, Arizona, a location where extreme temperatures, air pollution, and active transport come together for a large (~1.7 million people) and growing population. A specific bus route was selected that services numerous communities, including disadvantaged communities. Our study approach investigates the ability of mobile, lower-cost sensors to identify pockets of elevated heat and air pollution to aid targeted mitigation efforts. In the following subsections, we introduce the study area and discuss the rationale for selecting the bus route on which the experiment is conducted. We also explain the design of the experiment, the instruments used, and the data collection and analysis procedures.

2.1. Study area and selected route

The Phoenix metro region is one of the nation's largest and fastest-growing urban areas in terms of population and land area (US Census, 2020; Levitt and Eng, 2021). The metropolitan area, which is in a subtropical desert, is known for its extreme climate with low precipitation and high temperatures. During the summer, temperatures can reach over 110ºF (43ºC). In addition, the American Lung Association, which tracks citizen exposure to unhealthy pollutants, ranks Phoenix among the most polluted metro regions for its air quality (American Lung Association, 2022). Ozone, short-term particle pollution, and year-round particle pollution are all major concerns in the region. Extreme temperatures and poor air quality in the metro area pose major health concerns to residents.

The Maryvale Circulator was chosen for this study specifically because it serves a neighborhood that is home to one of the metropolitan area's most vulnerable populations (Chow et al., 2012). The Maryvale neighborhood is an urban village in the City of Phoenix with a population of over 200,000 people. More than a third of Maryvale's population is made up of communities of color. The area's median household income is approximately 15% lower than the state median. Furthermore, one-quarter of the population is reportedly living below the federal poverty level, which is two times higher than the state average (ADHS, 2021). Therefore, the study findings are intended to inform planning processes aimed at improving the well-being of residents in neighborhoods with high rates of vulnerable populations.

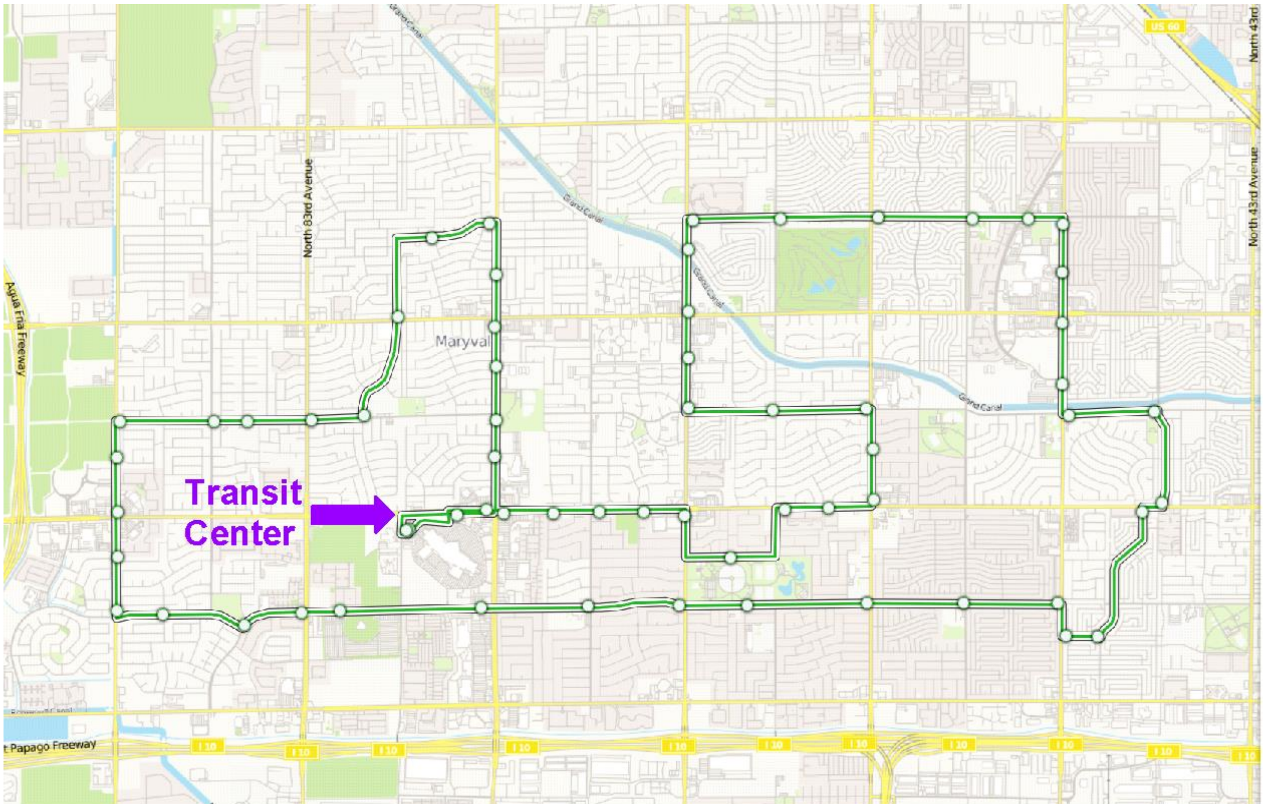

Figure 1: Maryvale urban village of Phoenix, AZ and the Maryvale Circulator bus route (Moovit, 2022)

The Mary Circulator route loops through the neighborhood, connecting passengers to schools, businesses, and other points of interest. Within an area of 16 square miles (41 km^2), it takes about 2 hours to complete a 20-mile route including 28 stops (Valley Metro, 2022) – see Figure 1. Bus headway is 30 minutes from 6 am to 8 pm, seven days a week. It also starts and ends at a transit center where passengers can connect to a variety of bus routes to travel to Downtown Phoenix and other destinations. As a result, unlike many other bus routes that traverse the entire metropolitan area and only pass through a single community on rare occasions, the Mary Circulator allows for more sampling at the local/village level. Given the vulnerability and environmental justice concerns of the community, the Maryvale Circulator provides an ideal route for sampling.

2.2. Instruments and vehicle setups

This study's data was primarily collected using three instruments to measure temperature, measure air pollution (specifically PM_{10}), and GPS location. The instruments, their primary measurements, and their sample rates are summarized in Table 1.

Table 1. Instruments used in this study

Instrument	Measurement	Accuracy	Response time	Sample rate
Kestrel DROP D2 Temperature & Humidity Data Logger	Temperature ($°C$)	$\pm 0.2\ °C$	5 sec	1 min
Aeroqual Series 500 - Portable Air Quality Monitor	PM_{10}	$\pm 0.002\ mg/m^3$ $+15\ \%\ of\ reading$	5 sec	1 min
Tracki Real-Time GPS Tracker	Coordinates	15 meters (~50 feet)	—	1 min

A portable air temperature logger was used to collect temperature data (Kestrel DROP D2 Wireless Temperature & Humidity Data Logger). These sensors record temperature with an accuracy of ±0.5ºC at 0.1ºC resolution and span the range of -10ºC to 55ºC (Kestrel, 2016). Throughout the study period, the Kestrel sensor was used to record the mean daily ambient temperature (°C), relative humidity (percent), dew point (°C), and heat stress index (°C).

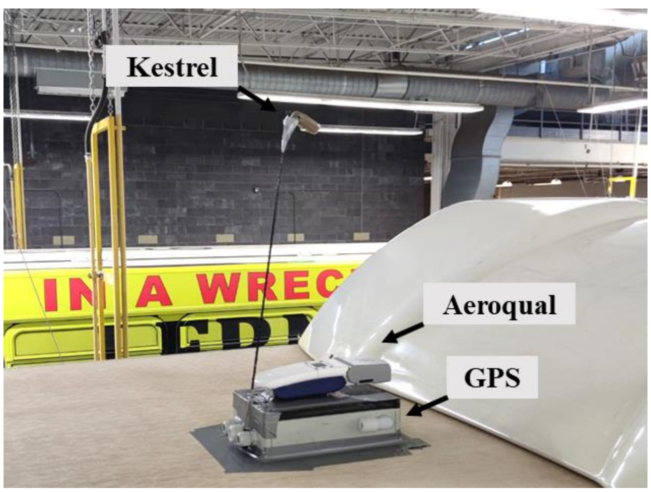

Figure 2. Vehicle setup with the three sensors (Kestrel, Aeroqual, GPS) on the top, front of the bus: the Aeroqual is located on the surface, adjacent to the GPS whereas the Kestrel sensor was hung from a 24-inch-long antenna to minimize the potential for radiant heat from the vehicle.

An Aeroqual Series 500 Portable Air Quality Monitor and an attached PM sampling head were used to measure PM_{10} concentrations. These hand-held sensors are widely used in the field for a variety of scientific applications (e.g., see reviews by McKercher et al., 2017 and Snyder et al., 2013) and can detect 30 different pollutants when combined with modular sampling heads for different pollutant types. A rechargeable lithium battery powers the sensors, which can last up to 20 hours with a PM head. In this study, the day-long battery life enabled data collection along the chosen route, which runs from 6 a.m. to 8 p.m. Finally, a Tracki Real-Time GPS Tracker was used to collect real-time GPS coordinates of the buses on which the sensors are mounted. The collected location coordinates were linked with air temperature and PM_{10} measurements based on their timestamps. The three instruments (Kestrel, Aeroqual, GPS) were then strategically mounted to the top of the front part of the vehicle (above the driver) -- see Figure 2. This location was chosen because it was as far away from the vehicle tailpipe (located in the lower rear part of the vehicle) as possible to mitigate potential influence from the bus exhaust and waste heat. Potential interference from the bus exhaust was further mitigated by the fact that data was only collected while the vehicle was in motion, which also ensures sensor ventilation – see Figure 2 for the specific positioning of each sensor.

2.3. Calibration of mobile sensors with stationary sensors

Temperature and air quality sensors were both calibrated by their manufacturers. However, because the climate in Arizona is very hot and dry in the summer, additional validation was necessary. To accomplish this, portable sensors were placed next to stationary weather and air quality monitoring stations. The measurements taken by mobile sensors were then compared to those taken by stationary sensors. For the comparisons, stationary sites were selected that are located nearest to the bus routes. The meteorological station at Papago Park was used for the temperature comparisons from June 6 to 11, 2021 (CAP-LTER, 2022). PM_{10} comparisons were conducted from June 10 to June 16, 2021, at the Central Phoenix Station Air Monitoring Site (Maricopa County Air Quality Department, 2022). The meteorological conditions during the validation activities were typically hot and dry for the summer months in Phoenix and consistent with the hot and dry meteorological conditions during our data collection efforts that took place in July and August 2021.

The calibration process displayed instrument reliability. The comparisons of portable temperature and PM_{10} sensors to stationary sites are shown in Figure 3. The sample sizes for temperature and PM_{10} comparisons are 562 and 799, respectively. An ordinary least square line is fitted in each subplot to show the magnitude of the correlation between the portable sensor and stationary sensor readings. The accuracy rate (R^2) is found to be 0.97 and 0.81, respectively for the temperature and PM_{10} comparisons. The temperature readings by the Kestrel sensor were within the range of ±4ºC as compared to readings by the stationary sensors located at the site. However, the portable PM_{10} sensor reported consistently and considerably lower readings than the stationary PM_{10} sensor.

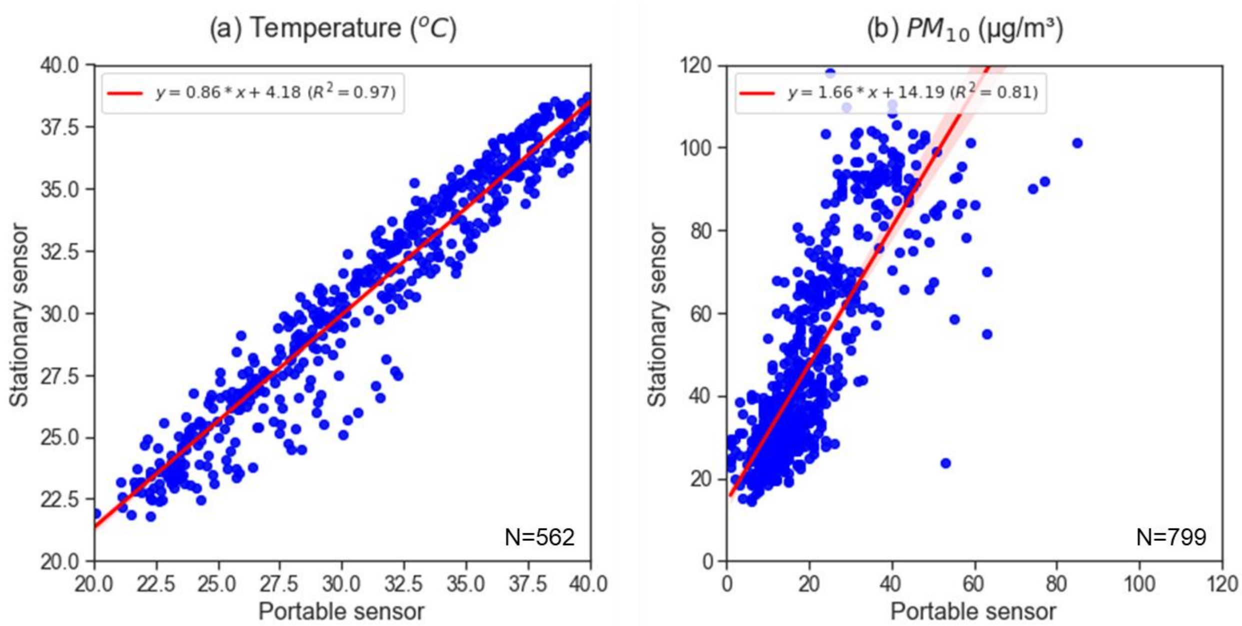

Figure 3. Completed comparisons for calibration of the portable (a) air temperature and (b) PM_{10} sensors to stationary sensors at the meteorological station and county reference monitor, respectively

This under-reporting issue with the PM_{10} sensor could be attributed to several factors. First, low-cost PM sensors, which use lasers as air particle counters, are less able to sense coarse particles as they fall out of the air faster than finer particles; thus, the area's distinct summer climate with a high proportion of coarser dust particles may have contributed to the under-reporting (Clements et al., 2013; Sousan et al., 2017). Second, because the airflow rate of low-cost sensors is significantly lower than that of reference stationary monitors, low-cost sensors pull much less air, resulting in less accurate measurements. Finally, low-cost sensors read particulate matter using different technology than reference stationary monitors, which may have also contributed to the under-reporting. Despite these limitations and differences, the portable PM_{10} sensor closely follows the stationary sensor's trend with a relatively high accuracy rate (R^2=0.81) – suggesting that low-cost sensors can still provide meaningful insights in the context of this study (as supported by Clements et al., 2017). Without any further calibration efforts, the study is carried out with the portable PM_{10} sensor to account for the spatial and temporal PM_{10} differences along the selected bus route.

2.4. Data collection and analysis

The timestamps on each sensor were first properly matched at the start of each experiment day to assure the spatial correctness of data points. The sensors were then mounted on top of the buses that operated on the days of the experiment. Since the main focus of the study was on understanding the spatiotemporal patterns of extreme heat and pollutant concentrations, the study period was limited to the summer months and to the warmer days with no rain. For this reason, the analysis period is limited to morning and afternoon hours when heat exposure is the highest (EPA, 2022). Data collection, accordingly, took place on July 8, 2021, and August 19, 2021, with sensors deployed in one vehicle on each experiment day.

After removing the data points with missing GPS coordinates, the data were plotted on a map to investigate the spatial variability of temperature and PM_{10} conditions for the study day. As the circulator bus service makes a full trip in a two-hour period, the data were further analyzed for two-hour tours in creating spatial maps for each tour. The goal was to observe the temporal consistency throughout the day and identify the pockets of elevated heat and air pollution on the route. Here, a distinction is made between temperature and PM_{10} observations. For temperature observations, a stationary weather monitoring site[†] (located at Phoenix Sky Harbor Airport) is used to account for the temporal variability of temperature within the day. The temperature data reported by the monitoring site on a minute-by-minute basis is subtracted from each observation recorded along the route. Thus, a location where consistently higher temperatures are observed as compared to the weather monitoring site is considered a potential hotspot of extreme heat. However, this method is not used for PM_{10} analysis because such temporal variability for PM_{10} is difficult to

[†] It should be noted that the Sky Harbor International Airport weather monitoring station is not the same one that was used for calibration. The reasoning is that the calibration station is not only further away from Maryvale Neighborhood than the airport station, but it also reports temperatures every 10 minutes. And because our experiment is designed to account for temporal variation on a minute-by-minute basis, we did not use this station to account for temporal variation in our experiment. On the other hand, we were unable to use the airport monitoring station for calibration purposes, simply because we did not have access to it. However, because the primary goal of the calibration effort was to see if the portable mobile sensor used in the study reported any unusual temperature readings, this does not pose a significant challenge to the study.

obtain. That is, PM_{10} readings were reported exactly as they were, reflecting the raw conditions in that specific location and time.

Furthermore, the land-use characteristics of each location are considered in the analysis to attribute the spatial temperature differences observed along the route. In doing so, the correlation matrix between temperature differences and the landform characteristics obtained at 50-meter resolutions are computed. The data for land-form characteristics were generated by the Central Arizona-Phoenix Long-Term Ecological Research (CAP LTER) program using the 2015 National Agriculture Imagery Program (NAIP) data (Zhang and Turner, 2020). The statistical significance of the correlation coefficients in the matrix is also determined at a 95% confidence level by performing standard hypothesis testing, with the null hypothesis assuming that the correlation coefficient is equal to zero.

3. RESULTS

3.1. Temperature analysis findings

When mobile temperature readings are compared to fixed temperature measurements, considerable neighborhood-scale variations emerge. Table 2 presents summary statistics for mobile and stationary temperature observations on the experimental days. Temperatures in the Maryvale neighborhood are modestly higher (~1°C on average) than those from the nearby stationary site. Peak temperatures in the area, on the other hand, were much higher, reaching nearly 49°C on July 8 and 39°C on August 19 (where maximum temperatures recorded by the stationary site at the airport were measured at 44°C and 36ºC). On a point-by-point basis, the largest difference between mobile and stationary measurements is 6.3°C and 5.1°C on July 8 and August 19, respectively.

Table 2. Summary statistics: Stationary versus mobile temperature measurements

Statistics	Experiment day					
	July 8, 2021			August 19, 2021		
	Mobile	Stationary	Difference	Mobile	Stationary	Difference
Minimum (ºC)	35.5	35.0	-2.4	28.3	26.1	–1.8
Maximum (ºC)	48.8	43.9	6.3	38.5	36.1	5.1
Average (ºC)	41.1	40.4	0.7	33.18	32.6	0.6

Figure 4 shows the temporal variability of temperature data recorded by the mobile sensor and the stationary weather monitoring site on both experiment days. At first glance, this point-by-point comparison appears to suggest that the mobile sensor closely follows the daily patterns of the temperature conditions recorded by the stationary monitoring site. However, a deeper examination of the figure reveals that the mobile sensor, for the most part, records hotter temperatures than what is reported by the nearby stationary monitoring site — with temperature differences exceeding 4°C on various occasions over the trial days. This shows that certain areas of the neighborhood might be significantly warmer, necessitating a thorough spatial investigation to identify potential hotspots.

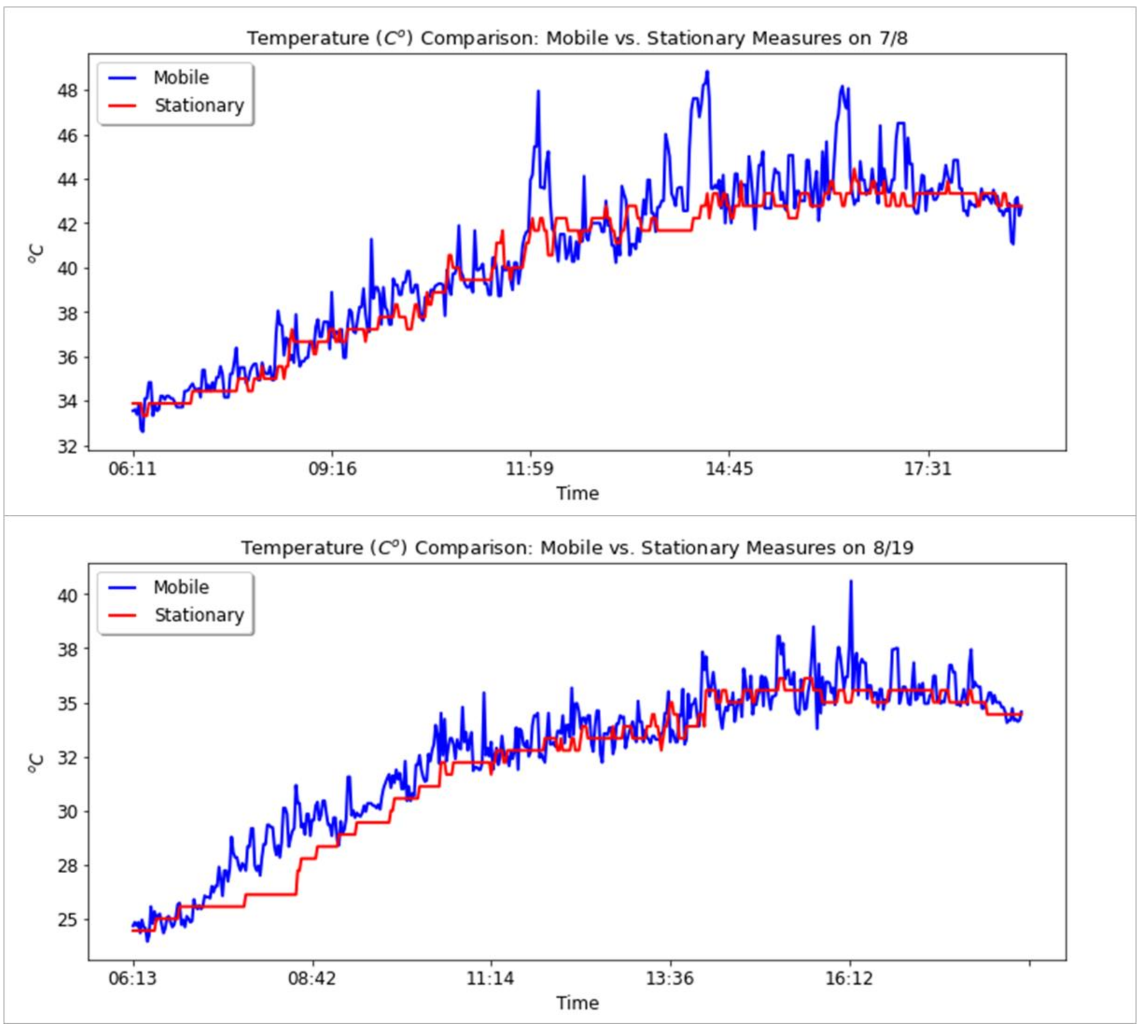

Figure 4. Mobile sensor measurements compared to measurements taken at stationary monitoring site on two days: July 8, 2021, and August 19, 2021

From the perspective of human health and heat risk mitigation, the higher maximum temperatures in Maryvale are particularly important. A maximum temperature of 48.8ºC in Maryvale compared to the airport (stationary) maximum of 43.9ºC can equate to a difference between "Extreme Danger" (the most severe category) and "Danger" with respect to local heat index charts and safety recommendations (ADHS, 2011). On relatively cooler days, maximum temperatures in Maryvale of 38.5ºC compared to stationary temperatures of 36.1ºC translate to a difference between "Danger" and "Extreme Caution" health effects and recommendations.

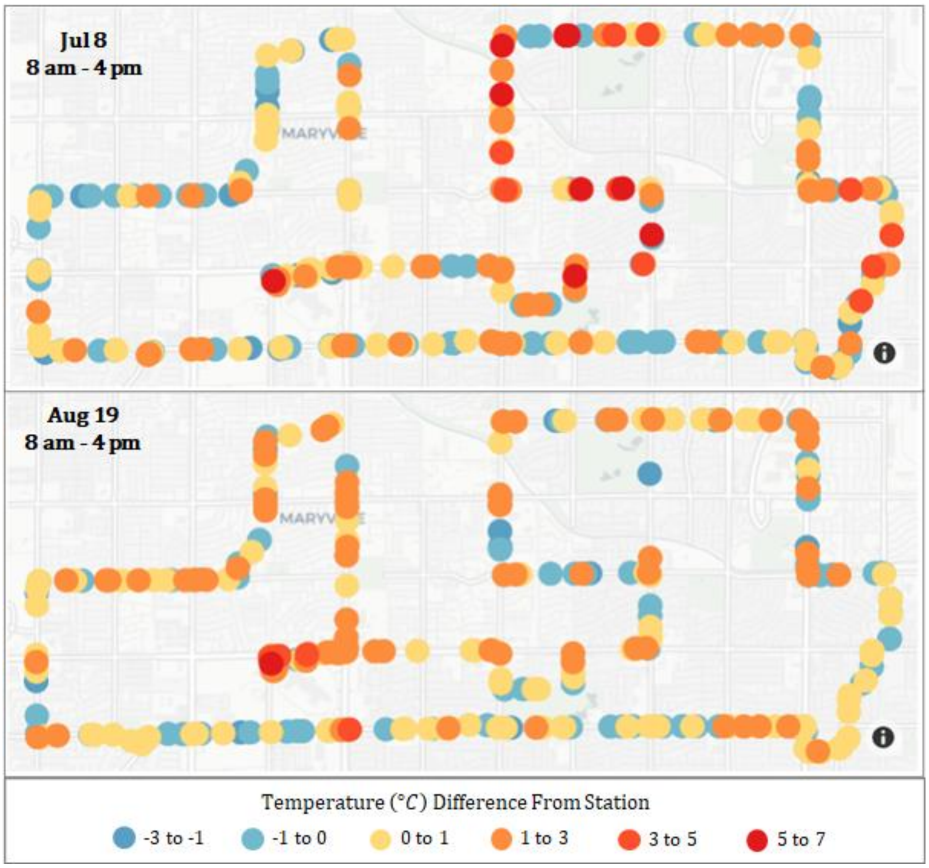

Figure 5. Geolocated temperature differences from 8 a.m. to 4 p.m. on July 8, 2021, and August 19, 2021

The spatial variation of temperature is investigated by mapping the geolocated temperature data recorded by the Maryvale Circulator as it travels along its route. Instead of employing the raw temperature data recorded by the mobile sensor, temperature differences (ºC) between the mobile sensor and the nearby monitoring site are used to account for temporal variability of temperature over the course of the observation period. Within the relatively confined geographic area of the Maryvale neighborhood, there is considerable variability as temperature differences (between mobile and stationary) ranged from -2.4ºC to +6.3ºC. Figure 5 depicts the geolocated temperature differences from 8 a.m. to 4 p.m. for the two experiment days. Colors of blue reflect mobile measurements that are lower than stationary readings, while shades of yellow, orange, and red represent mobile readings that are greater than stationary measurements. On both days, several locations and corridors along the Maryvale Circulator route are noticeably warmer than the rest of the route, indicating that these are potential hotspots where pedestrians, bicyclists, and transit riders (walking to and waiting at stops) are exposed to greater heat impacts than the rest of the population.

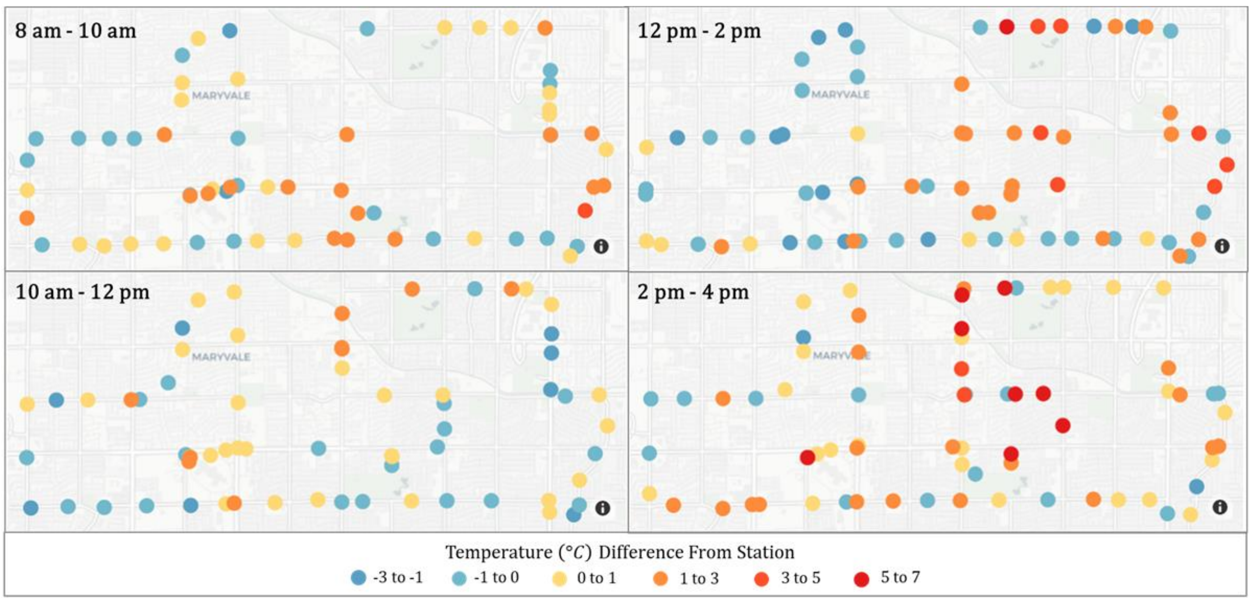

Figure 6. Temperature differences (ºC) from the station for four tours on July 8, 2021

Furthermore, these hotspots are investigated to determine if they remain warmer throughout the day. As the Maryvale Circulator takes roughly 2 hours to complete the entire 20-mile tour, the study period is separated into 2-hour-long tours to ensure it covers the entire route with adequate data points. Figure 6 depicts the temperature variations on four tours (8 am to 10 am; 10 am to 12 pm; 12 pm to 2 pm; and 2 pm to 4 pm) over the course of July 8, 2021[‡]. Again, the values in the figure show temperature differences from the nearby weather station and are color-coded in the same way. This tour-based comparison in Figure 6 reveals that many of the

[‡] The hotspots on the tour-based analysis appeared on both days, however, to conserve space, we opted to show it only for July 8, 2021.

hotspots seen in Figure 5 remain warmer no matter what time of day the temperature is monitored, illustrating the potential of mobile sensors to detect spatial temperature variability at finer scales.

In addition to providing insights into how temperature conditions at the human scale tend to change within the neighborhood, this study also investigates the role of the built environment as a potential contributor to this spatial variation in temperature (and air quality). For example, Figure 7 shows a specific location that was observed to have elevated temperature and air pollution (see Section 3.2) values across nearly all observation periods. This area has a shopping mall, and a transit center, and is near the intersection of two major streets. The large concentration of asphalt and traffic associated with this location are possible contributors to the elevated levels of temperature and air pollution, which in turn may contribute to greater risks – especially to people who utilize the transit center in this area to connect to other places.

Figure 7. Built environment of a potential hotspot (clearly shows excessively paved surface)

Beyond this anecdotal approach, the relationship between the built environment and warmer areas is investigated statistically. For every temperature recording along the route, the ratios of soil, shrub, pool, cropland, building, trees, and grass are extracted at 50-meter resolutions, and their connections with temperature differences are evaluated. Higher temperature differences along the route, as shown in Table 3, are positively and significantly correlated with the ratio of roads, but negatively correlated with the ratios of buildings, trees, and croplands. Along with the expectations, trees and croplands absorb and store less heat than artificial surface materials such as concrete and asphalt, therefore leading to lower temperatures. Furthermore, the finding that trees and buildings are inversely correlated with higher temperature differences matches prior studies (Parket et al., 2021; EPA, 2022b) that point to their role in reducing surface and air temperature through shading.

Table 3. Correlation between temperature differences and land-form characteristics

Correlation		**Land-form Characteristics**							
		Soil	**Shrub**	**Road**	**Pool**	**Cropland**	**Building**	**Tree**	**Grass**
Temperature Differences (°C)	Pearson's r	0.04	-0.01	0.09*	-0.03	-0.09*	-0.16**	-0.17**	0.01
	p-value	0.39	0.086	0.03	0.45	0.04	0.00	0.00	0.89

Note: * $p < 0.05$, ** $p < 0.01$

According to the temperature analysis, residents in the Maryvale neighborhood, who are among Arizona's most vulnerable populations, are exposed to more heat in the absence of adequate urban vegetation and mitigation strategies, a finding that adds to the literature on disproportionate heat exposure experienced by underrepresented groups (Nesbitt et al., 2019; Hsu et al., 2021). Furthermore, the findings suggest that the temporal and spatial variation detected by mobile sensors does not occur randomly due to instrument noise, since the built environment partially explains some of this variability. This shows that mobile sensors can not only complement stationary weather monitoring sites but also uncover key details about heat exposure experienced at the human scale.

3.2 Air quality analysis

Similar to temperature, considerable variability in air pollution was observed across the Maryvale neighborhood, with PM_{10} concentrations ranging from 3 μg/m^3 to over 150 μg/m^3. The raw PM_{10} values recorded by the mobile sensor are mapped along the Maryvale Circulator. Figure 8 shows the concentration maps depicting geo-recorded PM_{10} data from 8 a.m. to 8 p.m. on July 8 and August 19, 2021. This allows us to see the human-scale spatial and temporal variation of PM_{10} within the neighborhood. Unlike the maps that show temperature differences, the concentration maps (Figure 8) are generated using a kernel density algorithm to visualize raw PM_{10}

measurements in units of micrograms per cubic meter of air ($\mu g/m^3$). Points on the figures are color-coded, with shades of blue and green representing lower PM_{10} concentrations and shades of yellow, orange, and red representing higher PM_{10} concentrations.

Several locations along the Circulator route appear to have higher PM_{10} concentrations than other locations. A closer examination of these locations reveals that they are located near road intersections or along major roadways, implying that increased vehicular movement activity exacerbates PM_{10} in these areas. Relatedly, the mobile sensing device provides a new level of fidelity in identifying when and where PM_{10} concentrations approach unsafe levels for human health. According to the Environmental Protection Agency (EPA, 2022a), the 24-hour average of PM_{10} concentrations in a given area must not reach 150 $\mu g/m^3$ more than once per year on average over three years to be considered safe. Even though the 24-hour average was below the EPA threshold on both experiment days, PM_{10} concentrations exceeded 150 $\mu g/m^3$ at least once on August 19. However, the nearest air quality monitoring station reports a maximum PM_{10} value of 38 $\mu g/m^3$ on that day. These insights underscore the disproportionate nature by which residents are exposed to potentially hazardous conditions, as well as the fact that stationary data alone may not reveal these conditions. It also signifies the capability of mobile sensing technologies to detect locations with deteriorated air quality and overcome some of the geospatial limitations of stationary air quality sites.

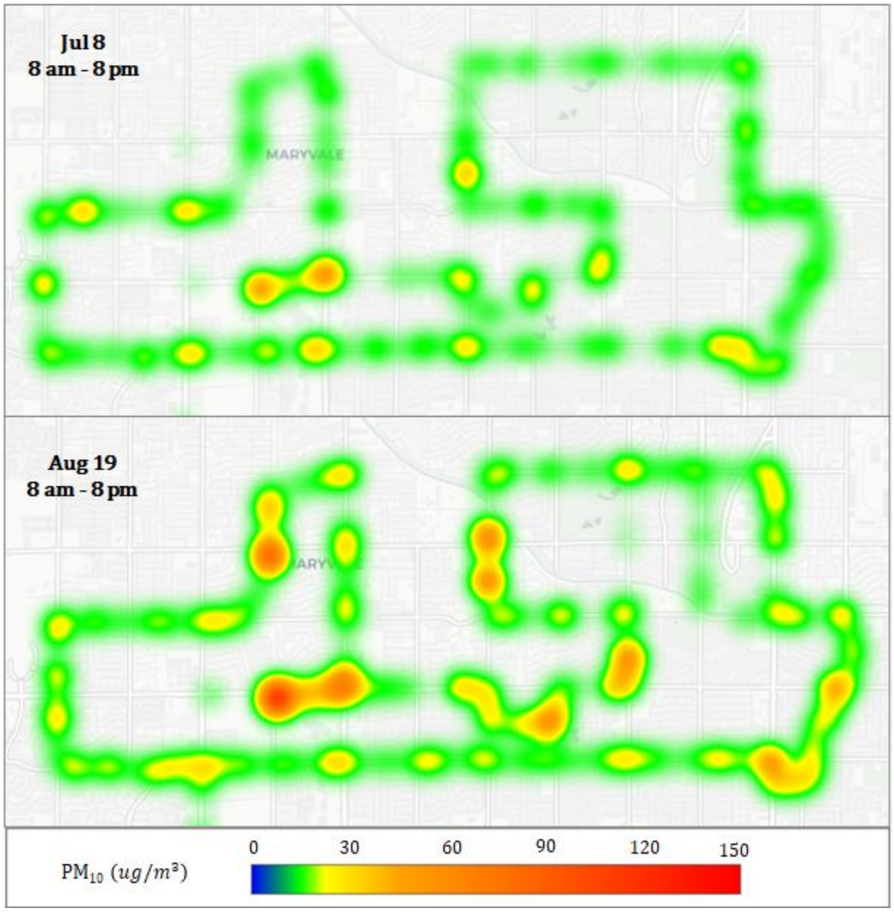

Figure 8. PM_{10} concentrations on July 8, 2021, and August 19, 2021

The level of spatial heterogeneity and variability mobile sensors are able to capture is further underscored when mobile sensor measurements along the Circulator route were compared to data collected at the nearest stationary site. Figure 9 shows the PM_{10} concentrations measured by the closest stationary regulatory monitoring site administered by the Maricopa County Air Quality Department (with 5-min intervals) and the mobile sensor (with 1-min intervals) on both experiment days. Considering their different locations within the city, the objective of this figure is not to conduct a one-to-one comparison of the two sites because we would expect them to differ. Instead, the takeaway should be the relative differences in ranges they exhibit and what they might imply about the intraurban variability of air pollution.

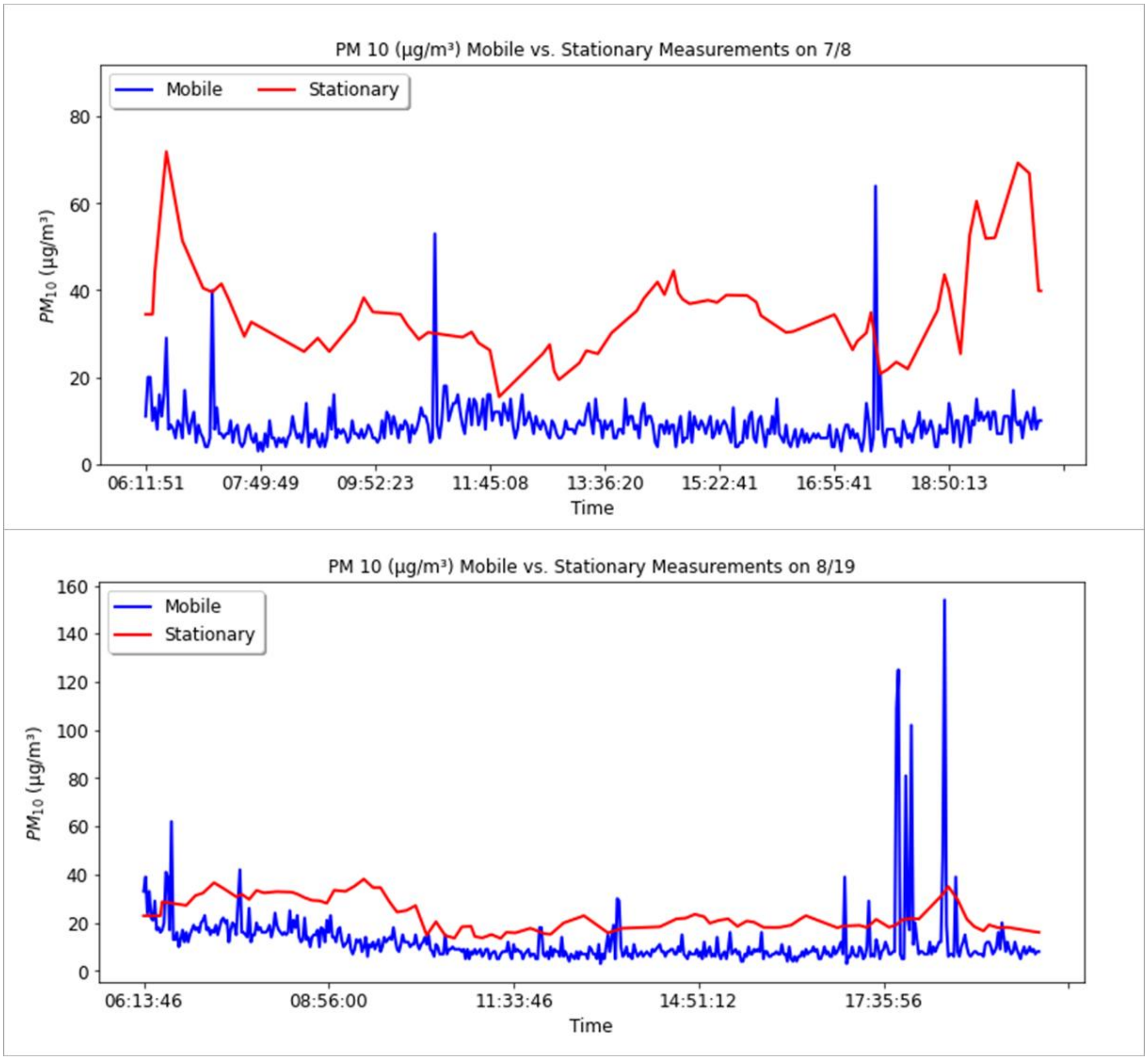

Figure 9. PM_{10} measurements from mobile sensor and stationary monitoring site on July 8 and August 19, 2021

For August 19, the range of mobile recordings (3 to 154 μg/m^3) is significantly wider than that of stationary recordings (14 to 38 μg/m^3), as shown in Figure 9. This begs the question of why the mobile sensor reports a greater range. Is it because mobile sensors are low-cost and low-quality, resulting in higher instrument noise? Or is it because mobile readings obtained at numerous sites provide more information about an area's air quality conditions than a stationary site collecting data at a single location? The validation of the mobile sensor against the stationary monitor revealed a significantly strong correlation between the two sensors, with an R^2 of 0.81 (see Figure 3); therefore, we believe the latter is more plausible. This suggests that, despite the sensors at air monitoring stations having possibly higher precision, the information gained from these sensors is constrained to the exact site of the stations; consequently, the measurements collected at these stations may not be able to generalize to a larger area. Conversely, while mobile sensors appear to underestimate PM_{10} concentrations, they provide valuable information on air quality conditions at the human scale, making them well suited to inform neighborhood mitigation efforts.

3.3 Limitations

We acknowledge that analysis focusing on one neighborhood, in one city, in a relatively short period, may not be sufficient to reach definitive conclusions that are applicable across a wide suite of contexts. There are also some general limitations associated with mobile sensors. Due to the nature of mobile measurements, sampling frequency at a given location is substantially shorter as compared to stationary monitoring sites – thus, resulting in a short snapshot at a certain location in time (Van den Bossche et al., 2015; Li et al., 2018). These sensors also have longer response times to stimuli (with a minimum of a few seconds) and are often prone to temporal drift, cross-sensitivity, and weather dependence (Snyder et al., 2013; Arfire et al., 2016). As a result, the data collected by these sensors is usually less reliable than that collected by standard stationary sensors. Fine-scale sampling enabled by mobile sensing technology thus comes at the cost of diminished measurement precision and accuracy.

To elaborate more on these trade-offs, limitations primarily relate to the lower inherent accuracy and higher sensor lag times of the mobile sensors (compared to more expensive and more sophisticated sensors). Mobile sensor measurements may also be impacted by the transient nature of the environment in which they were deployed. For example, when traveling in specific directions at specific times of day, the Kestrel sensors may have been exposed to direct sunlight, resulting in higher-than-expected temperature readings. We took a variety of steps to account for and minimize the influence of these limitations (see Section 2). However, it is possible that some may have persisted in various forms. For example, given response times and sample rates for the sensors, movement of the vehicle during measurement, and inherent uncertainty with the GPS tracker, we anticipate the location of our measurements to have an uncertainty range of at least 15 meters. Similarly, based on calibration and validation activities, there is the possibility that PM_{10} measurements from the mobile sensors may be underestimating actual concentrations. To address this, regular and consistent calibration is recommended for any extended deployment of mobile sensors to ensure that there isn't drift in sensor readings and accuracy over time.

Despite the possible limitations and uncertainties described above, we do not expect that they will have a significant impact on the results and insights from our analysis. This is primarily due to our focus on identifying relative differences in temperature and air quality across time and/or space, rather than measuring raw values. To that end, we want to emphasize that, for the time-being, mobile sensors should be viewed as a complement to the existing stationary network, not a replacement. In particular, they are well-suited for identifying hotspots and relative heterogeneity in environmental conditions. At that point, more robust "field-test" sensors could be deployed to confirm the specific location and conditions of trouble areas, as well as any targeted interventions.

To facilitate the expanded adoption of sensor-embedded transit systems, we highlight some logistical challenges we faced due to battery and data storage limitations with the sensors. Sensor capacity constraints limited data collection to single-day (approximately 12 hours) deployments. This required twice-daily coordination between team members and our public transit partners (one for sensor deployment in the morning and another for sensor retrieval in the evening). This level of coordination may not be possible or feasible for other transit authorities in other locations. Fortunately, the continual development and increased availability of next-generation sensors will help mitigate these issues moving forward. In particular, sensors with longer battery lives, the ability to connect to on-board power supplies, and/or the ability for cloud-based storage/transmission of data will reduce coordination burdens in future endeavors and enable more continuous deployment and data collection.

4. DISCUSSIONS

For both temperature and air quality, our analysis underscores the value of looking at finer scales to truly appreciate (and address) exposure to hazards like extreme heat and air pollution. Our approach and results also highlight the potential for mobile sensing platforms to produce these finer-scale insights, especially regarding observing variability across and within neighborhoods. In the absence of finer-scale observations and considerations of geospatial heterogeneity, heat advisories/warnings and air quality standards based on information from stationary sites appear to be susceptible to under-representing the actual conditions to which people living and traveling in a specific community are exposed – see discussion of local heat indexes in Section 3.1 and discussion of EPA air quality standards in Section 3.2. With the expansion and increased adoption of mobile sensors, one can envision policies and actions that are attuned to the times and locations where exposure pathways are most prevalent. For example, revised air quality standards could be supported by measurements at the street or neighborhood scale (as opposed to the regional scale), and heat indices could be tailored to individual communities rather than having a uniform index for the entire urban area.

Related to the observed spatial and temporal variability, mobile sensors allow for the identification of specific "hotspots" where temperature and/or air pollution conditions are particularly elevated compared to other locations and/or times – both within neighborhoods and across cities. For example, the identification of the mall and co-located transit center as a hotspot for both temperature and air pollution could inform several actions and policies to mitigate risk from these hazards. Information about the elevated hazard levels could be shared with transit users (particularly those that frequently use the identified transit center), which in turn result in behavior changes (e.g., wearing a mask to reduce exposure to air pollution; altering travel times to avoid high exposure conditions). Similarly, the transit authority can ensure that the travel center is properly ventilated and cooled to minimize exposure to heat and air pollution for riders waiting for their bus. Additionally, city officials could develop policies (e.g., altering parking minimums in building codes) and/or incentives (e.g., rebates for planting trees and/or increasing pervious surfaces) to reduce the amount of asphalt and parking activity in the area.

Although certain "hotspots" appear to remain relatively persistent across time (e.g., Figure 7), others appear to shift within and between days (e.g., Figures 6 and 8). For example, the mall parking lot consistently shows up as a hotspot while the large shopping center in the northeast part of the sample area varies as a hotspot. Ultimately, the collective results and observations from the mobile data point to a more complex and nuanced understanding of temperature and air quality than current approaches and stationary measurements may provide. Hazard levels and exposure pathways vary widely across relatively confined geographic areas and shift over the course of time. Essentially, not all parking lots, intersections, and land cover are created equal when it comes to extreme heat and air pollution. Striving toward mobile and distributed sensor networks can help us better understand micro-climates and unpack how people experience (and are exposed to) their environments.

Transit-embedded mobile sensing platforms are not the only approach for increasing the fidelity by which we observe and respond to urban environmental hazards. One possible option would be to install more stationary towers throughout a given region. However, financial and space constraints limit the feasibility of this option. In the absence of constructing new stationary towers, mobile sensing platforms can supplement the existing monitoring network by allowing for targeted assessment of specific areas under specific conditions – especially as mobile sensors become increasingly accurate and affordable. Coupling sensing with transit systems shows promise for providing insights at these finer scales (e.g., transit stops, intersections, road segments). Mobile sensing platforms can also help address environmental justice and equity issues by providing supplemental monitoring in marginalized communities – especially in communities not well represented by the existing stationary monitoring network. For instance, transit riders often comprise potentially vulnerable populations (e.g., young, elderly, lower socio-economic standing) and typically have elevated exposure to hazards (due to walking to and waiting at transit stops). Sensor-embedded transit systems allow for the collection of information that is highly relevant to their specific routes and exposure pathways and enables more curated mitigation efforts. Additionally, sensor-embedded transit systems can complement the monitoring of the progress and effectiveness of localized heat and air pollution mitigation strategies. For example, if a city plants several trees in a specific area in an attempt to mitigate extreme heat and air pollution, sensor-embedded buses/trains along the tree-planting corridor could provide valuable before and after measurements of temperature and air quality to better quantify and track the effectiveness of the mitigation effort(s).

Finally, we appear to be moving toward a model of distributed technology that enables a level of cognition that we have not had previously. As small-scale sensors continue to become more accurate and affordable, one can envision a future where nearly every street corner, building, and vehicle is outfitted with connected temperature and air quality sensors. Until we reach that point, exploring and implementing sensor-embedding mobile platforms appears to be well positioned to provide some initial insights into the potential role and implications that this increased cognition can have on individual and collective decision-making. With a relatively small set of observations, we were able to identify new levels of nuance and refinement with respect to understanding localized exposure to and mitigation of extreme heat and air pollution. As follow-up research efforts collect more data (over longer periods of time, across more locations, for more hazards, and at increasingly finer scales), we can continue to move toward a finer-scale understanding of heat and air pollution in complex and heterogeneous urban environments. Ultimately, this refined understanding can help us shift from place-based to person-based exposure identification and mitigation which will be critical for equitably and effectively protecting the well-being of all urban residents.

5. CONCLUSION

This paper focuses on the efficacy of low-cost mobile sensors in uncovering the spatial and temporal variations of excessive heat and air pollution experienced at the street level. Low-cost temperature and air quality sensors were mounted on public transportation vehicles as part of an experiment to monitor fine-scale on-road heat and PM_{10} concentrations along a bus route in Phoenix, Arizona. The experiment results showed that mobile sensing platforms can provide a more in-depth and nuanced understanding of temperature and air quality conditions in urban areas than conventional approaches based on stationary monitoring data. Hazard levels and exposure pathways varied and shifted over the course of time across the relatively confined study area. Furthermore, the experiment results revealed that mobile sensors can be used to identify certain "hotspots" where temperature and/or air pollution levels are significantly higher than in other locations and/or times – both within neighborhoods and across cities.

Significant gaps remain in the quality of information concerning the risks associated with extreme heat and air pollution, as conditions continue to be typically monitored by a sparse network of stationary sensors that provide information at a large geographic scale. With portable sensors becoming more accurate and affordable, we may foresee a future in which air quality and meteorological conditions are continuously monitored at every street corner and building. Until we reach that point, equipping public transit vehicles with low-cost sensors and developing mobile sensing platforms can be an effective way to collect fine-grained heat and air quality data. This way, it is possible to enhance our understanding of urban microclimates and heat and air quality hazards that transit riders, bicyclists, and pedestrians experience, resulting in new insights and opportunities for targeted intervention.

ACKNOWLEDGMENTS

This research was sponsored by the Zimin Institute for Smart and Sustainable Cities at Arizona State University. The authors are thankful to Miguel A. Garcia from the City of Phoenix for assisting with vehicle setup, as well as Joshua Uebelherr, Ronald Pope, and Ben Davis from the Maricopa County Air Quality Department and Megan Gaitan and Quincy Stewart from the CAP LTER at Arizona State University for assisting with data collection/acquisition at air monitoring and weather stations.

AUTHOR CONTRIBUTIONS

The authors confirm contributions to the paper as follows: study conception and design: I. Batur, S. A. Markolf, and M. V. Chester; data collection: I. Batur, S. A. Markolf, and M. V. Chester; analysis and interpretation of results: I. Batur, S. A. Markolf, M. V. Chester, A. Middel, D. Hondula, and J. Vanos; draft manuscript preparation: I. Batur, S. A. Markolf, M. V. Chester, A. Middel, D. Hondula, and J. Vanos. All authors reviewed the results and approved the final version of the manuscript.

REFERENCES

ADHS - Arizona Department of Health Services, 2011. *Heat Index Chart with Health Effects and Safety Recommendations*. Available at: https://www.azdhs.gov/documents/preparedness/epidemiology-disease-control/extreme-weather/heat/Heat-Index-Chart.pdf (Accessed: 14 April 2022).

ADHS - Arizona Department of Health Services, 2021. *Maryvale Village Primary Care Area: 2020 Statistical Profile*. Available at: https://azdhs.gov/documents/prevention/health-systems-development/data-reports-maps/primary-care/maricopa/36.pdf (Accessed: 12 April 2022).

Alsina-Pagès, R.M., Hernandez-Jayo, U., Alías, F. and Angulo, I., 2016. Design of a mobile low-cost sensor network using urban buses for real-time ubiquitous noise monitoring. *Sensors*, *17*(1), p.57.

American Lung Association, 2022. *Most Polluted Cities | State of the Air*. Available at: https://www.lung.org/research/sota/city-rankings/most-polluted-cities (Accessed: 14 April 2022).

Anenberg, S.C., Haines, S., Wang, E., Nassikas, N. and Kinney, P.L., 2020. Synergistic health effects of air pollution, temperature, and pollen exposure: a systematic review of epidemiological evidence. *Environmental Health*, *19*(1), pp.1-19.

Arfire, A., Marjovi, A. and Martinoli, A., 2016. Mitigating slow dynamics of low-cost chemical sensors for mobile air quality monitoring sensor networks. In *International Conference on Embedded Wireless Systems and Networks* (No. CONF).

Barri, E.Y., Farber, S., Kramer, A., Jahanshahi, H., Allen, J. and Beyazit, E., 2021. Can transit investments in low-income neighbourhoods increase transit use? Exploring the nexus of income, car-ownership, and transit accessibility in Toronto. *Transportation Research Part D: Transport and Environment*, *95*, p.102849.

Baxter, L. K., Dionisio, K. L., Burke, J., Ebelt Sarnat, S., Sarnat, J. A., Hodas, N., ... & Özkaynak, H. (2013). Exposure prediction approaches used in air pollution epidemiology studies: key findings and future recommendations. *Journal of exposure science & environmental epidemiology*, 23(6), 654-659.

Brandsma, T. and Wolters, D., 2012. Measurement and statistical modeling of the urban heat island of the city of Utrecht (the Netherlands). *Journal of Applied Meteorology and Climatology*, *51*(6), pp.1046-1060.

CAP-LTER (Central Arizona–Phoenix Long-Term Ecological Research), 2022. *Weather stations: Papago Park and Lost Dutchman State Park*. Available at: https://sustainability-innovation.asu.edu/caplter/research/long-term-monitoring/weather-stations-papago-dutchman-state-park/ (Accessed: 12 April 2022).

Chen, Y., Jiang, W.M., Zhang, N., He, X.F. and Zhou, R.W., 2009. Numerical simulation of the anthropogenic heat effect on urban boundary layer structure. *Theoretical and applied climatology*, *97*(1), pp.123-134.

Chow, W.T., Chuang, W.C. and Gober, P., 2012. Vulnerability to extreme heat in metropolitan Phoenix: spatial, temporal, and demographic dimensions. *The Professional Geographer*, *64*(2), pp.286-302.

Clements, A.L., Fraser, M.P., Upadhyay, N., Herckes, P., Sundblom, M., Lantz, J. and Solomon, P.A., 2013. Characterization of summertime coarse particulate matter in the Desert Southwest—Arizona, USA. *Journal of the Air & Waste Management Association*, *63*(7), pp.764-772.

Clements, A.L., Griswold, W.G., Rs, A., Johnston, J.E., Herting, M.M., Thorson, J., Collier-

Oxandale, A. and Hannigan, M., 2017. Low-cost air quality monitoring tools: from research to practice (a workshop summary). Sensors, 17(11), p.2478.

Davis, R.E., Normile, C.P., Sitka, L., Hondula, D.M., Knight, D.B., Gawtry, S.P. and Stenger, P.J., 2010. A comparison of trajectory and air mass approaches to examine ozone variability. *Atmospheric Environment*, *44*(1), pp.64-74.

Eisenman, D.P., Wilhalme, H., Tseng, C.H., Chester, M., English, P., Pincetl, S., Fraser, A., Vangala, S. and Dhaliwal, S.K., 2016. Heat Death Associations with the built environment, social vulnerability and their interactions with rising temperature. *Health & place*, *41*, pp.89-99.

Elen, B., Peters, J., Van Poppel, M., Bleux, N., Theunis, J., Reggente, M. and Standaert, A., 2012. The Aeroflex: a bicycle for mobile air quality measurements. *Sensors*, *13*(1), pp.221-240.

Emmanuel, R. and Fernando, H.J., 2007. Urban heat islands in humid and arid climates: role of urban form and thermal properties in Colombo, Sri Lanka and Phoenix, USA. *Climate Research*, *34*(3), pp.241-251.

EPA - Environmental Protection Agency, 2022a. *NAAQS Table*. Available at: https://www.epa.gov/criteria-air-pollutants/naaqs-table (Accessed: 12 April 2022).

EPA - Environmental Protection Agency, 2022b. *Ultraviolet (UV) Radiation and Sun Exposure*. Available at: https://www.epa.gov/radtown/ultraviolet-uv-radiation-and-sun-exposure (Accessed: 12 April 2022).

EPA - Environmental Protection Agency, 2022c. *Using Trees and Vegetation to Reduce Heat Islands | US EPA*. Available at: https://www.epa.gov/heatislands/using-trees-and-vegetation-reduce-heat-islands (Accessed: 12 April 2022).

Fan, H. and Sailor, D.J., 2005. Modeling the impacts of anthropogenic heating on the urban climate of Philadelphia: a comparison of implementations in two PBL schemes. *Atmospheric environment*, *39*(1), pp.73-84.

Gil-Castineira, F., Gonzalez-Castano, F.J., Duro, R.J. and Lopez-Pena, F., 2008, July. Urban pollution monitoring through opportunistic mobile sensor networks based on public transport. In *2008 IEEE International Conference on Computational Intelligence for Measurement Systems and Applications* (pp. 70-74). IEEE.

Glass, K., Tait, P.W., Hanna, E.G. and Dear, K., 2015. Estimating risks of heat strain by age and sex: A population-level simulation model. *International journal of environmental research* *and public health*, *12*(5), pp.5241-5255.

Hankey, S. and Marshall, J.D., 2015. Land use regression models of on-road particulate air pollution (particle number, black carbon, PM2. 5, particle size) using mobile monitoring. *Environmental science & technology*, *49*(15), pp.9194-9202.

Hondula, D.M., Davis, R.E., Saha, M.V., Wegner, C.R. and Veazey, L.M., 2015. Geographic dimensions of heat-related mortality in seven US cities. *Environmental research*, *138*, pp.439-452.

Hondula, D. M., Davis, R. E., & Georgescu, M., 2018. Clarifying the connections between green space, urban climate, and heat-related mortality. American journal of public health, 108(S2), S62-S63.

Hsu, A., Sheriff, G., Chakraborty, T. and Manya, D., 2021. Disproportionate exposure to urban heat island intensity across major US cities. *Nature communications*, *12*(1), pp.1-11.

Ichinose, T., Shimodozono, K. and Hanaki, K., 1999. Impact of anthropogenic heat on urban climate in Tokyo. *Atmospheric Environment*, *33*(24-25), pp.3897-3909.

Jamil, M.S., Jamil, M.A., Mazhar, A., Ikram, A., Ahmed, A. and Munawar, U., 2015. Smart environment monitoring system by employing wireless sensor networks on vehicles for pollution free smart cities. *Procedia Engineering*, *107*, pp.480-484.

Jerrett, M., Arain, A., Kanaroglou, P., Beckerman, B., Potoglou, D., Sahsuvaroglu, T., ... & Giovis, C. (2005). A review and evaluation of intraurban air pollution exposure models. Journal of Exposure Science & Environmental Epidemiology, 15(2), 185-204.

Kaivonen, S. and Ngai, E.C.H., 2020. Real-time air pollution monitoring with sensors on city bus. *Digital Communications and Networks*, *6*(1), pp.23-30.

Karner, A., Hondula, D.M. and Vanos, J.K., 2015. Heat exposure during non-motorized travel: Implications for transportation policy under climate change. *Journal of Transport & Health*, *2*(4), pp.451-459.

Kestrel, 2016. *DROP Wireless Environmental Data Loggers: Certificate of Conformity*. Available at: https://cdn.shopify.com/s/files/1/0084/9012/files/DROP_Certificate_of_Calibaration.pdf?14953145177891566479 (Accessed: 12 April 2022).

Krayenhoff, E. S., Broadbent, A. M., Zhao, L., Georgescu, M., Middel, A., Voogt, J. A., ... & Erell, E, 2021. Cooling hot cities: a systematic and critical review of the numerical modelling literature. Environmental Research Letters, 16(5), 053007.

Kumar, P., Morawska, L., Martani, C., Biskos, G., Neophytou, M., Di Sabatino, S., ... & Britter, R. (2015). The rise of low-cost sensing for managing air pollution in cities. Environment international, 75, 199-205.

Kuras, E.R., Hondula, D.M. and Brown-Saracino, J., 2015. Heterogeneity in individually experienced temperatures (IETs) within an urban neighborhood: insights from a new approach to measuring heat exposure. *International journal of biometeorology*, *59*(10), pp.1363-1372.

Kuras, E.R., Richardson, M.B., Calkins, M.M., Ebi, K.L., Hess, J.J., Kintziger, K.W., Jagger, M.A., Middel, A., Scott, A.A., Spector, J.T. and Uejio, C.K., 2017. Opportunities and challenges for personal heat exposure research. *Environmental Health Perspectives*, *125*(8), p.085001.

Levitt, Z. and Eng, J., 2021. Where America's developed areas are growing: 'Way off into the horizon'. Available at: https://www.washingtonpost.com/nation/interactive/2021/land-development-urban-growth-maps/ (Accessed: 15 April 2022).

Li, X., Li, W., Middel, A., Harlan, S.L., Brazel, A.J. and Turner Ii, B.L., 2016. Remote sensing of the surface urban heat island and land architecture in Phoenix, Arizona: Combined effects of land composition and configuration and cadastral–demographic–economic factors. *Remote Sensing of Environment*, *174*, pp.233-243.

Li, Z., Fung, J.C. and Lau, A.K., 2018. High spatiotemporal characterization of on-road PM2. 5 concentrations in high-density urban areas using mobile monitoring. *Building and Environment*, *143*, pp.196-205.

Lin, C.Y., Chen, F., Huang, J.C., Chen, W.C., Liou, Y.A., Chen, W.N. and Liu, S.C., 2008. Urban heat island effect and its impact on boundary layer development and land–sea circulation over northern Taiwan. *Atmospheric Environment*, *42*(22), pp.5635-5649.

Lupiani, J., 2021. *HEAT KILLS: Extreme heat kills hundreds of people each year*. Available at: https://www.ktnv.com/news/heat-kills-more-than-600-people-died-each-year-because-of-extreme-heat (Accessed: 12 April 2022).

Makar, P.A., Gravel, S., Chirkov, V., Strawbridge, K.B., Froude, F., Arnold, J. and Brook, J., 2006. Heat flux, urban properties, and regional weather. *Atmospheric environment*, *40*(15), pp.2750-2766.

Mallia, D.V., Mitchell, L.E., Kunik, L., Fasoli, B., Bares, R., Gurney, K.R., Mendoza, D.L. and

Lin, J.C., 2020. Constraining urban CO2 emissions using mobile observations from a light rail public transit platform. *Environmental Science & Technology*, *54*(24), pp.15613-15621.

Maricopa County Air Quality Department, 2022. *Maricopa County Interactive Air Quality Map Guide*. Available at: https://alert.fcd.maricopa.gov/alert/Google/v3/airnow.html (Accessed: 12 April 2022).

Maricopa County Public Health, 2021. *Heat-Associated Deaths in Maricopa County, AZ Final Report for 2021*. Available at: https://www.maricopa.gov/ArchiveCenter/ViewFile/Item/5494 (Accessed: 10 October 2022).

Marjovi, A., Arfire, A. and Martinoli, A., 2015, June. High resolution air pollution maps in urban environments using mobile sensor networks. In *2015 International Conference on Distributed Computing in Sensor Systems* (pp. 11-20). IEEE.

McKercher, G.R., Salmond, J.A. and Vanos, J.K., 2017. Characteristics and applications of small, portable gaseous air pollution monitors. *Environmental Pollution*, *223*, pp.102-110.

McKercher, G. R., & Vanos, J. K. (2018). Low-cost mobile air pollution monitoring in urban environments: a pilot study in Lubbock, Texas. Environmental technology, 39(12), 1505-1514.

Middel, A., Häb, K., Brazel, A.J., Martin, C.A. and Guhathakurta, S., 2014. Impact of urban form and design on mid-afternoon microclimate in Phoenix Local Climate Zones. *Landscape and urban planning*, *122*, pp.16-28.

Middel, A., Nazarian, N., Demuzere, M., and Bechtel, B., 2022. Urban Climate Informatics – an emerging research field, *Frontiers in Environmental Science, pp. 10:867434. doi: 10.3389/fenvs.2022.867434.*

Miller, D.J., Actkinson, B., Padilla, L., Griffin, R.J., Moore, K., Lewis, P.G.T., Gardner-Frolick, R., Craft, E., Portier, C.J., Hamburg, S.P. and Alvarez, R.A., 2020. Characterizing elevated urban air pollutant spatial patterns with mobile monitoring in Houston, Texas. *Environmental Science & Technology*, *54*(4), pp.2133-2142.

Middel, A., & Krayenhoff, E. S., 2019. Micrometeorological determinants of pedestrian thermal exposure during record-breaking heat in Tempe, Arizona: Introducing the MaRTy observational platform. Science of the total environment, 687, 137-151.

Miller, D. J., Actkinson, B., Padilla, L., Griffin, R. J., Moore, K., Lewis, P. G. T., ... & Alvarez, R. A. (2020). Characterizing elevated urban air pollutant spatial patterns with mobile monitoring in Houston, Texas. Environmental science & technology, 54(4), 2133-2142.

Mitchell, L.E., Crosman, E.T., Jacques, A.A., Fasoli, B., Leclair-Marzolf, L., Horel, J., Bowling, D.R., Ehleringer, J.R. and Lin, J.C., 2018. Monitoring of greenhouse gases and pollutants across an urban area using a light-rail public transit platform. *Atmospheric Environment*, *187*, pp.9-23.

Moovit, 2022. *Line Route MARY*. Available at: https://moovitapp.com/phoenix_az-746/lines/MARY/236476/1608951/en?customerId=4908&ref=2&poiType=line (Accessed: 12 April 2022).

Myint, S.W., Zheng, B., Talen, E., Fan, C., Kaplan, S., Middel, A., Smith, M., Huang, H.P. and Brazel, A., 2015. Does the spatial arrangement of urban landscape matter? Examples of urban warming and cooling in Phoenix and Las Vegas. *Ecosystem Health and Sustainability*, *1*(4), pp.1-15.

National Weather Service, 2020. *Weather Related Fatality and Injury Statistics*. Available at: https://www.weather.gov/hazstat/ (Accessed: 12 April 2022).

Nazarian, N., Krayenhoff, S., Bechtel, B., Hondula, D., Paolini, R., Vanos, J.K., Cheung, T., Chow, W.T.L., de Dear, R., Jay, O. and Lee, J.K., 2021. Integrated Assessment of Urban Overheating Impacts on Human Life.

Nesbitt, L., Meitner, M.J., Girling, C., Sheppard, S.R. and Lu, Y., 2019. Who has access to urban vegetation? A spatial analysis of distributional green equity in 10 US cities. *Landscape and Urban Planning*, *181*, pp.51-79.

Oke, T.R., Mills, G., Christen, A. and Voogt, J.A., 2017. *Urban climates*. Cambridge University Press.

Park, Y., Guldmann, J.M. and Liu, D., 2021. Impacts of tree and building shades on the urban heat island: combining remote sensing, 3D digital city and spatial regression approaches. *Computers, Environment and Urban Systems*, *88*, p.101655.

Phillips, A.M., Barboza, T., Vives, R. and Greene S., 2021. *California extreme heat deaths show climate change risks - Los Angeles Times*. Available at: https://www.latimes.com/projects/california-extreme-heat-deaths-show-climate-change-risks/ (Accessed: 12 April 2022).

Rahman, Md Mostafijur, Rob McConnell, Hannah Schlaerth, Joseph Ko, Sam Silva, Frederick W. Lurmann, Lawrence Palinkas et al. "The Effects of Co-Exposure to Extremes of Heat and

Particulate Air Pollution on Mortality in California: Implications for Climate Change." *American Journal of Respiratory and Critical Care Medicine* ja (2022).

Shi, Y., Katzschner, L., & Ng, E., 2018. Modelling the fine-scale spatiotemporal pattern of urban heat island effect using land use regression approach in a megacity. Science of the Total Environment, 618, 891-904.

Snyder, E.G., Watkins, T.H., Solomon, P.A., Thoma, E.D., Williams, R.W., Hagler, G.S., Shelow, D., Hindin, D.A., Kilaru, V.J. and Preuss, P.W., 2013. The changing paradigm of air pollution monitoring. *Environmental science & technology*, *47*(20), pp.11369-11377.

Sousan, S., Koehler, K., Hallett, L. and Peters, T.M., 2017. Evaluation of consumer monitors to measure particulate matter. *Journal of aerosol science*, *107*, pp.123-133.

Steinle, S., Reis, S., & Sabel, C. E. (2013). Quantifying human exposure to air pollution—Moving from static monitoring to spatio-temporally resolved personal exposure assessment. *Science of the Total Environment*, 443, 184-193US Census, 2020. *Southern and Western Regions Experienced Rapid Growth This Decade*. Available at: https://www.census.gov/newsroom/press-releases/2020/south-west-fastest-growing.html (Accessed: 15 April 2022).

Valley Metro, 2022. *Phoenix Mary Circulator*. Available at: https://www.valleymetro.org/maps-schedules/mary (Accessed: 12 April 2022).

Van den Bossche, J., Peters, J., Verwaeren, J., Botteldooren, D., Theunis, J. and De Baets, B., 2015. Mobile monitoring for mapping spatial variation in urban air quality: Development and validation of a methodology based on an extensive dataset. *Atmospheric Environment*, *105*, pp.148-161.

Viggiano, M., Busetto, L., Cimini, D., Di Paola, F., Geraldi, E., Ranghetti, L., ... & Romano, F. (2019). A new spatial modeling and interpolation approach for high-resolution temperature maps combining reanalysis data and ground measurements. Agricultural and Forest Meteorology, 276, 107590.

Xie, X., Semanjski, I., Gautama, S., Tsiligianni, E., Deligiannis, N., Rajan, R. T., ... & Philips, W. (2017). A review of urban air pollution monitoring and exposure assessment methods. ISPRS International Journal of Geo-Information, 6(12), 389.

Wang, J., Kou, L., Kwan, M. P., Shakespeare, R. M., Lee, K., & Park, Y. M. (2021). An Integrated Individual Environmental Exposure Assessment System for Real-Time Mobile Sensing in

Environmental Health Studies. Sensors, 21(12), 4039.

Whiteman, C.D., Hoch, S.W., Horel, J.D. and Charland, A., 2014. Relationship between particulate air pollution and meteorological variables in Utah's Salt Lake Valley. *Atmospheric Environment*, *94*, pp.742-753.

Wu, C. D., Zeng, Y. T., & Lung, S. C. C. (2018). A hybrid kriging/land-use regression model to assess PM2. 5 spatial-temporal variability. Science of the Total Environment, 645, 1456-1464.

Zhang, Y., and Turner, B. L., 2020. Land-cover mapping of the central Arizona region based on 2015 National Agriculture Imagery Program (NAIP) imagery. https://sustainability-innovation.asu.edu/caplter/data/view/